Available online at www.sciencedirect.com
SCIENCE DIRECT
Journal of Photochemistry and Photobiology A: Chemistry 180 (2006) 88–100
Journal of Photochemistry and Photobiology A:Chemistry
www.elsevier.com/locate/jphotochem

Electron transfer and intersystem crossing processes in new dyes based on 1*H*-pyrazolo[3,4-*b*]quinoxaline Effect of temperature and solvent polarity on the CT fluorescence

Marek Mac [a,*], Andrzej Danel [b], Anna Wisła [b], Andrzej Karocki [a], Robert Królicki [a]

[a] *Faculty of Chemistry, Jagiellonian University, 30-060 Kraków, Ingardena 3, Poland*
[b] *Academy of Agriculture, 30-059 Kraków, Mickiewicza 24/28, Poland*

Received 11 February 2005; received in revised form 26 September 2005; accepted 28 September 2005
Available online 2 November 2005

Abstract

Three dyes containing the 1*H*-pyrazolo[3,4-*b*]quinoxaline moiety have been synthesized and investigated as novel fluorophores exhibiting charge transfer fluorescence. The effect of changing temperature and solvent polarity on CT fluorescence of these compounds was investigated by steady-state and time-resolved fluorescence methods. Detailed investigation of the influence of temperature on charge transfer fluorescence band shape indicates the importance of the intramolecular vibrational mode of medium frequency in the radiative back electron transfer process.

The second part of the paper deals with the intersystem crossing process leading to the population of the lowest triplet state of molecules. We found that population of the lowest molecular triplet state of 1*H*-pyrazolo[3,4-*b*]quinoxaline (**I**) in *n*-hexane proceeds via thermally activated process $^1LE \Rightarrow T_n$ followed by the fast internal conversion $T_n \Rightarrow T_1$. In polar solvents where the emitting singlet state has a CT character the reaction sequence $^1CT \Leftrightarrow {}^3CT \Rightarrow T_1$ seems to be not operative in the triplet state population. One possible explanation bases on the fact that increasing polarity of the solvent reduces the energy gap between the ^3CT and T_1 and in consequence reduces the electron transfer process occurring in normal Marcus region. Another possible explanation bases on the supposition that the intersystem crossing occurs only from the locally excited singlet state(^1LE). The emitting singlet state having a CT character possesses an admixture of the locally excited singlet state (π,π^*) which contribution decreases when the solvent polarity increases due to rising up the energy gap between the states. A direct $^1LE \Rightarrow T_1$ intersystem crossing is less probable in solvents not containing heavy atom and this fact seems to be responsible for the lack of phosphorescence of the investigated compounds at 77 K.

Keywords: Pyrazolo[3,4-*b*]quinoxalines; Fluorescence; Electron transfer; Intersystem crossing; Heavy atom effect; Solvent effect; Temperature effect

1. Introduction

The charge transfer fluorescence of azarenes was a subject of many investigations [1–10] due to their potential applicability for light-emitting devices (LEDs) [11]. Many azarene compounds exhibit a dual fluorescence which means that emission of these dyes contains two better or less resolved fluorescence bands, which differ in their solvent polarity dependence. The primary electron transfer process occurring in the excited state forms a diradical structure, containing radical ions, i.e. a structure with large dipole moment. The charge transfer emission (long-wave fluorescence) is a result of the radiative charge transfer process, leading finally to recovering the ground state of the dye. The last process is characterized by several parameters, which may be recovered from the CT fluorescence band shape analysis [12,13]. Such a model was adopted for explanation of the dual fluorescence of biaryls [14,15], aryl derivatives containing aromatic amines [2,16], bimolecular exciplexes [17], etc. The charge transfer character of the long-wave fluorescence is sufficiently proven by a large Stokes shift of the fluorescence, by temperature dependence of the fluorescence spectra, by transient absorption measurements and by time-dependent fluorescence experiments.

In this work the novel nitrogen-containing aromatic compounds, based on 1*H*-pyrazolo[3,4-*b*]quinoxaline skeleton which exhibit the CT fluorescence were studied (Fig. 1). We investigated the effect of changing solvent polarity, temperature

* Corresponding author.

1010-6030/$ – see front matter © 2005 Elsevier B.V. All rights reserved.
doi:10.1016/j.jphotochem.2005.09.027

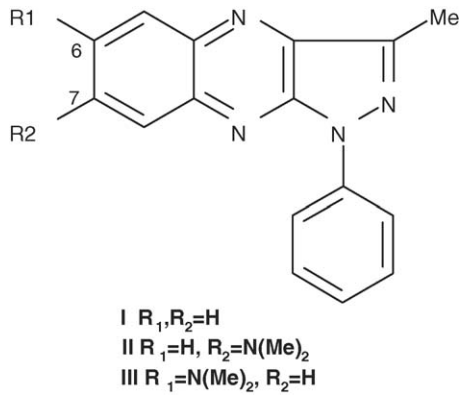

Fig. 1. Chemical structures of the investigated compounds.

and the existence of external heavy atom effect using these compounds. The results are discussed in terms of modern electron transfer theories.

It should be noted that for the compounds investigated here only one fluorescence band is observed in solvents of medium and high polarities, which indicates that the very fast and irreversible charge transfer process occurs in the excited singlet state (**I**) or the charge transfer state is populated directly via excitation (**II** and **III**).

On the other hand, for many aromatic molecules the population of the lowest triplet state (intersystem crossing process) occurs via the thermally activated process $S_1 \Rightarrow T_n$ followed by the very fast internal conversion $T_n \Rightarrow T_1$. In such cases the low-temperature phosphorescence may be not observed. We found such sequence of processes in our cases. The low-temperature phosphorescence is detected only in solvents containing heavy atom (iodine) where a direct $^1LE \Rightarrow T_1$ intersystem crossing is accelerated by the external heavy atom effect.

2. Experimental

The detailed synthesis of the investigated compounds will be published in an additional paper.

2.1. Synthesis of 1H-pyrazolo[3,4-b]quinoxalines

3-Methyl-1-phenyl-1*H*-pyrazolo[3,4-*b*]quinoxaline (**I**) and 6-*N,N*-dimethylamino-3-methyl-1-phenyl-1*H*-pyrazolo[3,4-*b*]-quinoxaline (**III**) were prepared by reductive cyclization of 5-chloro-3-methyl-4-nitro-1-phenylpyrazole with aromatic amines under microwave heating (Scheme 1).

7-*N,N*-Dimethylamino-3-methyl-1-phenyl-1*H*-pyrazolo[3,4-*b*]quinoxaline (**II**) was prepared according to the method described in the literature [18] (Scheme 2).

To synthesize 1*H*-pyrazolo[3,4-*b*]quinoxalines we applied the method, which was used in the synthesis of phenazines. In 1974 Bacon and Hamilton [19] obtained phenazines by thermal cyclization of 2-nitrophenylendiamines by iron(II) oxalate with lead shots.

The reaction conditions in the case of phenazines gave moderate yields of desired compounds. We used the same reduction compound (iron(II) oxalate) but in the sulfolane solution instead of lead shot. The reaction occurred in boiling solvent and was finished after 3–5 min.

Melting points (uncorrected) were measured on a Mel-Temp Apparatus II (capillary). NMR spectra were recorded on a Varian (Mercury 300) spectrometer at 25 °C. Column chromatography was carried out on Merck silica gel 60 (70–230 mesh) and Merck aluminium oxide 90 (70–230 mesh, **II**–**III** activity according to Brockman). Materials were purchased from Merck and Aldrich. A household microwave oven Whirpool AKL 535 (800 W) was used operating at 2450 MHz and at 20% of full power. TLC monitoring of the reaction was performed on silica gel 60 F_{254} plates (Merck) developed with chloroform.

5-Chloro-3-methyl-4-nitro-1-phenylpyrazole was prepared according to Khan and Freitas [20].

2.2. Synthesis of 1H-pyrazolo[3,4-b]quinoxalines—general procedure

Equimolecular amounts of 5-chloro-3-methyl-4-nitro-1-phenylpyrazole (0.01 mol, 2.38 g), aniline (0.01 mol, 0.93 g; or 1.36 g *N,N*-dimetyl-1,4-phenylenediamine) and iron(II) oxalate dihydrate (0.01 mol, 1.8 g) in sulfolane (10 ml) were heated in a microwave oven for 5 min. The hot solution was filtered to remove inorganic residue and washed with ethanol. The pyrazoloquinoxalines were precipitated with water. After drying the compounds were purified on aluminium oxide with chloroform as an eluent. The product was crystallized from toluene.

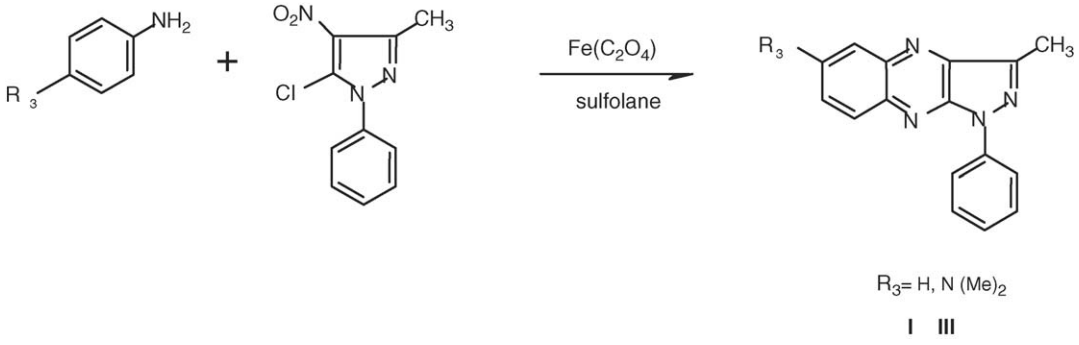

Scheme 1. Synthesis of 3-methyl-1-phenyl-1*H*-pyrazolo[3,4-*b*]quinoxaline (**I**) and 6-*N,N*-dimethylamino-3-methyl-1-phenyl-1*H*-pyrazolo[3,4-*b*]quinoxaline (**III**).

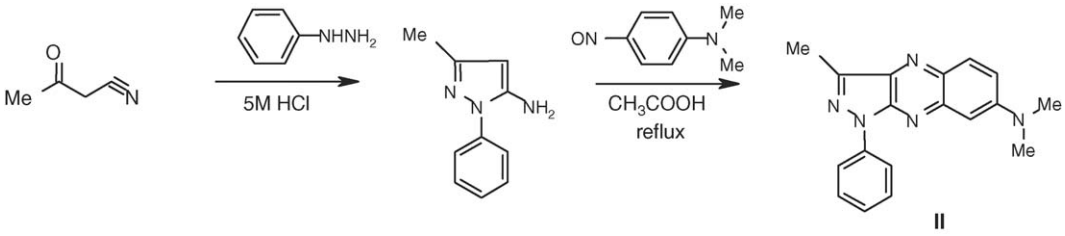

Scheme 2. Synthesis of 7-*N,N*-dimethylamino-3-methyl-1-phenyl-1*H*-pyrazolo[3,4-*b*]quinoxaline (**II**).

2.3. 3-Methyl-1-phenyl-1H-pyrazolo[3,4-b]quinoxaline (*I*)

Yellow crystals (47% yield): m.p. 130–131 °C. Anal. Calcd. for $C_{16}H_{12}N_4$: C 73.83%; H 4.65%; N 21.52%. Found: C 73.75; H 4.32; N 21.11. ^{1}H NMR (300 MHz, $CDCl_3$): δ (ppm), J(Hz): 8.51 (d, J = 7.4, 2H, 2′,6′-$H_{1\text{-Ph}}$); 8.35 (dd, J = 8.7, J' = 1.2, 1H, 8-H); 8.27 (dd, J = 8.5, J' = 0.8, 1H, 5-H); 7.91 (t, J = 1.6, 1H, 6-H); 7.80 (t, J = 6.9, 1H, 7-H); 7.63 (t, J = 7.9, 2H, 3′,5′-$H_{1\text{-Ph}}$); 7.37 (t, J = 7.7, 1H, 4-$H_{1\text{-Ph}}$); 2.93 (s, 3H, 3-CH_3).

2.4. 6-N,N-Dimethylamino-3-methyl-1-phenyl-1H-pyrazolo[3,4-b]quinoxaline (*III*)

Red crystals (27% yield): m.p. 187–188 °C. Anal. Calcd. for $C_{18}H_{17}N_5$: C 71.27%; H 5.65%; N 23.08%. Found: C 71.94; H 5.01; N 22.58. MS (*m/z*): 302.9 (100%); 301.9 (21.97%); 304.0 (21.14%). ^{1}H NMR (300 MHz, $CDCl_3$): δ (ppm), J (Hz): 8.47 (d, J = 8.3, 2H, 2′,6′-$H_{1\text{-Ph}}$); 8.08 (d, J = 9.3, 1H, 8-H); 7.63–7.55 (m, 4H, 5-H, 7-H, 3′,5′-$H_{1\text{-Ph}}$); 7.32 (t, J = 7.4, 1H, 4-$H_{1\text{-Ph}}$); 3.21 (s, 6H, Me_2N–); 2.88 (s, 3H, 3-CH_3).

2.5. Spectral and time-resolved measurements

The solvents *n*-hexane (Hex), toluene (Tol), dibutyl ether (DBE), tetrahydrofuran (THF), ethyl bromide (EtBr), ethyl iodide (EtI), dichloromethane (MeCl), acetone (Ac), acetonitrile (ACN), dimethylformamide (DMF), propylene carbonate (PC), dimethyl sulfoxide (DMSO) were of spectroscopic grade and were used as received (all from Aldrich). All solvents do not show any traces of fluorescence. For fluorescence and transient absorption measurements the solutions of the dyes were degassed using the freeze–pump–thaw cycles. The sample concentration of the dyes for spectroscopic measurements is ca. 10^{-5} M (it refers to absorbances of ca. 0.2–0.3 at excitation wavelength in the fluorescence and the transient absorption measurements).

Fluorescence measurements were done on a home-built spectrofluorimeter and a time-correlated single photon counting arrangement, described previously [15]. For time-resolved fluorescence measurements as excitation source a picosecond diode laser (IBH-UK) (λ = 400 nm, 70 ps pulse duration) was used. For steady-state fluorescence measurements a 365 or 405 nm line of medium-pressure mercury lamp was used. The temperature fluorescence measurements were done using a high- and low-temperature cryostat (Oxford Instruments, DN1704). The fluorescence quantum yields measurements were determined with quinine sulphate in water (Φ_{fl} = 0.55) as an actinometer.

Flash photolysis kinetic studies were carried out with the use of the LKS 60 Spectrometer from Applied Photophysics for detection and Nd:Yag laser for excitation (Surlite I-10 from Continuum) operating in third mode (355 nm, max 100 mJ pro pulse). Absorbance changes were monitored using a 150 W xenon lamp supplied with the pulse unit, and the photomultiplier tube R 628. The data were recorded on the digital storage oscilloscope HP 54522 A with the 0.5 ns time resolution and transferred to a computer for the analysis.

2.6. Calculations

Electron transfer parameters were recovered using the CT fluorescence band shape analysis, described in previous papers [15]. For minimization the MINUITS procedure from the CERN Library was employed. We minimized the following function:

$$\mathrm{FCN} = \sum_i (I(\nu_i) - \mathrm{CT}(\nu_i))^2 \tag{1}$$

where $I(\nu_i)$ is the corrected for spectral sensitivity fluorescence profile whereas $\mathrm{CT}(\nu_i)$ is the predicted CT transition probability given by the Gould and Farid formula [13,17]:

$$\mathrm{CT}(\nu) = n^3\nu^3\left(\frac{n^2+2}{3}\right)^2\frac{64\pi^2}{3h^3}M^2\sum_{j=0}^{\infty}\frac{S^j}{j!}(4\pi\lambda_s kT)^{-1/2}\exp \times\left(-\frac{(\Delta G_{et} + jh\nu_v + \lambda_s + h\nu)^2}{4\lambda_s kT}\right) \tag{2}$$

where the parameters used in this equation have following meanings: M is the transition dipole moment, λ_s the solvent reorganization energy, ΔG_{et} the energy difference between the CT and ground states, S the displacement parameter, connected with the internal reorganization energy (λ_{in}) and the energy of the ring skeletal vibration ($h\nu_v$ = 1600 cm^{-1}) by the relation:

$$S = \frac{\lambda_{in}}{h\nu_v} \tag{3}$$

Solvent reorganization energy, which describes the motions of the solvent molecules during the charge transfer process, may be calculated using the formula [16]:

$$\lambda_s = \frac{\Delta\vec{\mu}^2}{4\pi\varepsilon_0 a^3}\left(\frac{\varepsilon_s - 1}{2\varepsilon_s + 1} - \frac{n^2-1}{2n^2+1}\right) \tag{4}$$

where $\Delta\vec{\mu} = \vec{\mu}_e - \vec{\mu}_g$ is the difference between the excited and ground state dipole moments, respectively, ε_0 the dielectric permittivity of the vacuum, and a is the radius of Onsager cavity. The parameters ε_s and n are the static dielectric constant and refraction index of the solvent.

It should be noted that upon normalization of the CT spectrum to its maximal intensity Eq. (2) converts into a simpler one:

$$\mathrm{CT}(\nu) = \nu^3 \sum_{j=0}^{\infty} \frac{S^j}{j!} \exp\left(\frac{(\Delta G_{et} + jh\nu_v + \lambda_s + h\nu)^2}{4\lambda_s kT}\right) \quad (5)$$

In a first attempt (crude estimation), we found that λ_{in} scatters around a mean value and does not show significant changes with varying solvent polarity. Therefore, we repeated the minimization with a fixed value of $\lambda_{in} = 0.137$ and 0.125 eV for molecules **II** and **III**, respectively (refined estimation). The accuracy of the fit has been checked by the analysis of the nondiagonal elements of the covariance matrix, yielded by the MINUITS package. These elements which describe the correlation of the estimated values (i.e. ΔG_{et}, λ_s and λ_{in}) are significantly reduced when the third parameter (λ_{in}) has been fixed in the refined estimation. It should be noted that the error of estimation of the parameters never exceeded 10% the values in the final minimizations.

3. Results

3.1. Fluorescence measurements

Absorption spectra of the compounds (**I**–**III**) are presented in Fig. 2.

We can see that the position of the long-wave absorption of **I** is very weakly dependent on solvent polarity, whereas that for **III** shows strong dependence. The absorption spectrum of **II** consists of two overlapping absorption bands, position of the first is not sensitive to solvent polarity (a) and that of the second one is red-shifted and solvent polarity dependent (b). Moreover, the position of the band which is not sensitive to solvent polarity

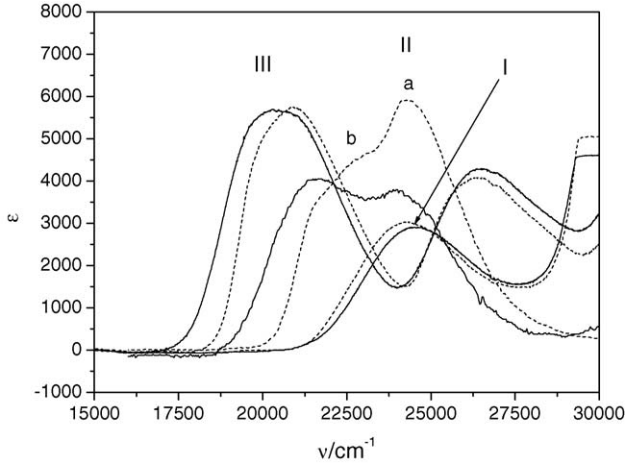

Fig. 2. Absorption spectra of **I**, **II** and **III** in DBE (broken lines) and DMF (solid lines).

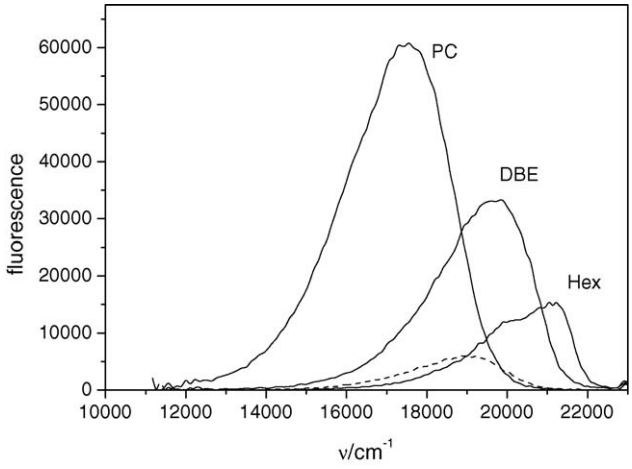

Fig. 3. Corrected fluorescence spectra of **II** in propylene carbonate (PC), dibutylether (DBE), hexane (Hex)—solid lines and in ethyl bromide (dashed line).

is approximately the same as the position of the 0–0 absorption band of **I**. We found that the extinction coefficient of band 'a' decreases when solvent polarity increases.

Fluorescence spectra of all the investigated compounds are much stronger dependent on solvent polarity as it is presented in Fig. 3.

We can see that fluorescence of **II** is broad and structureless in all solvents except *n*-hexane, for which a small vibrational structure is observed. Low intensity of the fluorescence spectrum of **II** in ethyl bromide indicates the existence of the external heavy atom effect. This effect will be discussed later.

Fluorescence of all the investigated compounds was also measured using time-resolved technique. The fluorescence decay times of these compounds together with other parameters obtained by steady-state fluorescence measurements are collected in Table 1.

The fluorescence behaviour of all the investigated compounds points out to its charge transfer character, i.e. the position of the fluorescence band, the fluorescence quantum yields and lifetimes depend strongly on polarity of the solvents. Moreover, this dependence is different for different molecules as it can be seen from Table 1. We can see that the fluorescence quantum yields and lifetimes of **I** decrease dramatically when solvent polarity increases, the small decrease of the above-mentioned values may be seen for compound **III** whereas for **II** we observe completely opposite situation, namely an increase of the fluorescence parameters with increasing solvent polarity. To explain these facts and to gather other fluorescence parameters we performed for these compounds the fluorescence (steady-state and time-resolved) measurements in selected solvents at different temperatures. The representative temperature dependent fluorescence spectra are presented below (Fig. 4).

Increasing temperature causes a hypsochromic shift of the position of the maximum of the spectral band except for the spectrum recorded at 140 K where the sample was frozen (thus the environment was nonpolar). Such a hypsochromic shift due

Table 1
Fluorescence lifetimes, quantum yields and position of the maximum of CT fluorescence for **I**, **II** and **III** at 293 K

Solvent	Compound **I**			Compound **II**			Compound **III**		
	τ_{fl} (ns)	Φ_{fl}	ν_{max} (cm^{-1})	τ_{fl} (ns)	Φ_{fl}	ν_{max} (cm^{-1})	τ_{fl} (ns)	Φ_{fl}	ν_{max} (cm^{-1})
Hex	23.0	0.31		1.8	0.11		19.2	0.37	
DBE	19.6	0.31	19970	4.8	0.33	19740	20.2	0.38	18120
THF	9.0	0.07?	18760	9.7	0.58	18680	20.0	0.39	18650
Tol	14.0	0.26	19340	5.0	0.43	19490	24.7	0.76	17850
EtBr	10.1	0.1	18770	2.3	0.3	19080	17.6	0.35	17380
ETI	5.32	0.06	18980	0.3	0.023	18980	4.5	0.08	17430
MeCl	5.92	0.053	18210	8.3	0.63	18640	23.7	0.37	17050
Ac	3.0	0.017	18160	12.6	0.7	18020	17.5	0.3	16290
ACN	1.58	0.017	17750	13.3	0.82	17760	16.5	0.26	16230
DMF	2.5	0.017	17910	12.0	0.9	17590	16.7	0.23	15960
PC	1.8	0.012	17780	12.1	0.89	17570	15.7	0.27	16020
DMSO	1.85	0.021	17690	10.4	0.92	17310	12.9	0.28	15640

The data refer to the degassed samples.

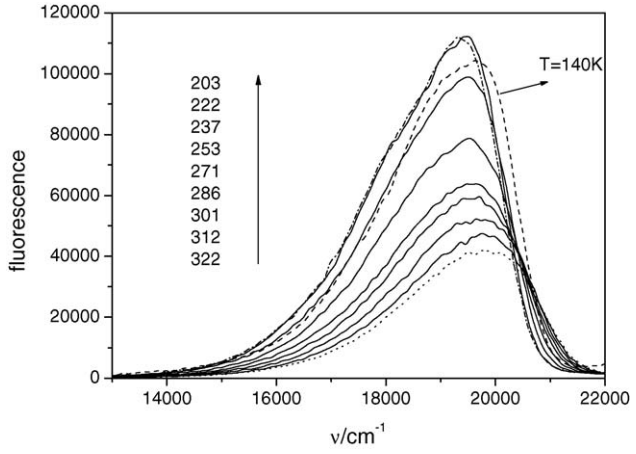

Fig. 4. Fluorescence spectra of **II** in DBE at different temperatures (from 140 to 322 K). The dashed line represents the spectrum taken at 140 K, where the sample was frozen. Increasing temperature causes a decrease of fluorescence intensity and blue shift of the position of the maximum of the spectra.

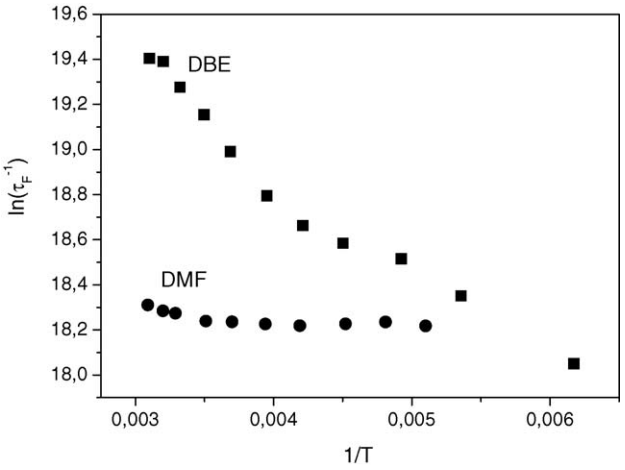

Fig. 5. Temperature dependence of the inverse of the fluorescence lifetimes of **II** in DBE and DMF.

to raising temperature was observed for all the investigated systems.

The dependence of the fluorescence lifetimes and quantum yields on temperature was very different for the investigated systems. Increasing temperature causes the decrease of the fluorescence lifetimes of all three compounds in nonpolar DBE. In strongly polar DMF the lifetimes of **II** are almost unaffected by changing temperature as pointed out in Fig. 5. An increase (small but distinct) of the fluorescence lifetime with increasing temperature was noticed for **I** and **III** in DMF and acetonitrile.

3.2. Transient absorption measurements

We observe the strong solvent polarity dependence of the fluorescence quantum yield of **II**. In nonpolar hexane an important deactivation channel of the emitting singlet state is operative, it may be the intersystem crossing process, yielding the molecules in their triplet state. Therefore we performed the transient absorption measurements of all compounds in solvents of different polarities. The examples of the transient absorption spectra are presented in Fig. 6.

The negative bands observed at 310 and 340 nm correspond to the bleaching of the ground state absorption bands and those in the range of 450–650 nm to the fluorescence of the compound in DBE. The signal at the UV region contains clearly two components which decay according to the first order kinetics with distinctly two different decay times. The short decay time matches exactly the fluorescence decay time whereas the second one is much longer (in microsecond region) and is affected by the presence of oxygen. Therefore, the short-time absorption may be attributed to the singlet–singlet absorption whereas the long-time absorption to the triplet–triplet absorption. We found that the intensities of the long-time absorption decrease when solvent polarity increases whereas the spectral distribution remains the same. In very polar PC only traces of long-lived absorption bands are observed as it is presented in Fig. 6. This indicates that the intersystem crossing yielding the molecules in the triplet state is less operative in polar solvents. This situation is common for other compounds investigated here (Fig. 7).

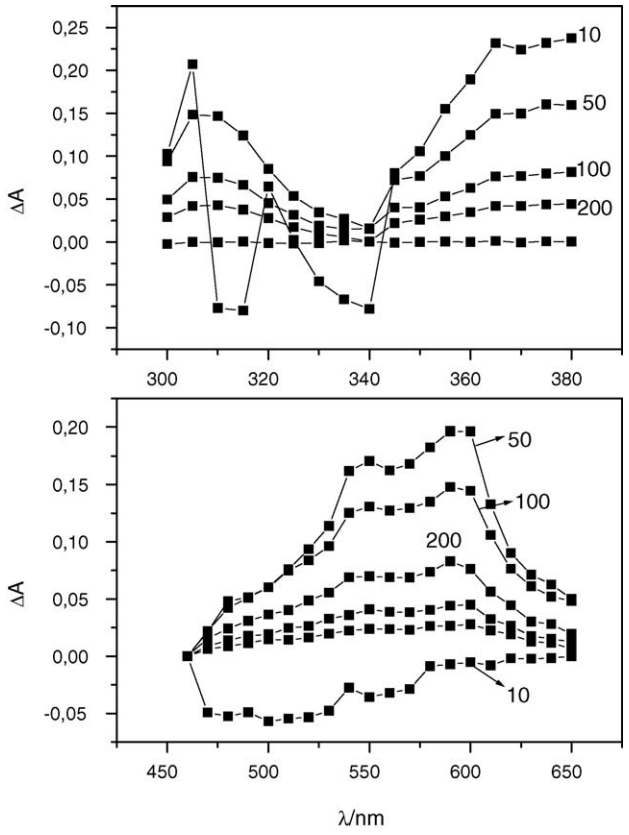

Fig. 6. Transient absorption spectra of **II** in *n*-hexane taken at different delay times (indicated in the figure in ns) after excitation by a 355 nm line of Nd:YAG laser.

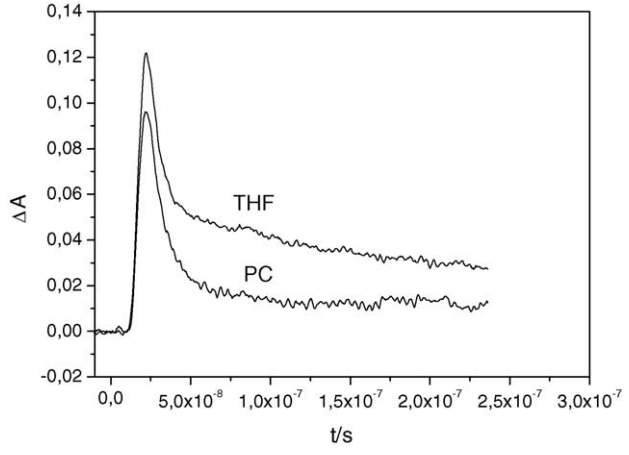

Fig. 7. Decay of the transient absorption signal of **II** at 340 nm in THF and PC (degassed samples).

4. Discussion

4.1. Analysis of the charge transfer fluorescence

All the presented above results indicate a charge transfer character of the excited singlet state which emits fluorescence in solvents of medium and higher polarities. Therefore, the fluorescence spectra of these compounds may be analysed in terms of the Marcus theory for radiative charge transfer process [12,13]. However, to perform a detailed analysis the differences between the excited state and the ground state dipole moments ($\Delta\vec{\mu}$) of these compounds should be known. For this purpose we applied the well-known Lippert–Mataga method [21]. Below the Lippert–Mataga plot for **II** is presented.

The excited state dipole moments are calculated according to the following equation:

$$\nu_{abs} - \nu_{fl} = \frac{\Delta\vec{\mu}^2}{2\pi\varepsilon_0 hca^3}\left(\frac{\varepsilon_s - 1}{2\varepsilon_s + 1} - \frac{n^2 - 1}{2n^2 + 1}\right) + \text{constant} \quad (6)$$

where ν_{abs} and ν_{fl} are the spectral positions of the maximum of the CT absorption and equilibrated emission, respectively, the other parameters were already previously defined (Fig. 8).

To calculate the dipole moments enhancement ($\Delta\vec{\mu}$) of the investigated substances using Eq. (6) we need to know the cavity radius of the molecules. We assumed the value of 5.9 Å as an averaged value of this quantity on the basis of semiempirical calculations (Hyperchem). The ground state dipole moments were calculated using the Gaussian packet and provided the values of 1.4, 5.1 and 4.5 D for **I**, **II** and **III**, respectively. The differences between the excited state and the ground state dipole moments are estimated as 13.0 and 13.3 D for **II** and **III**, respectively. The small dipole moment of **I** is responsible for the lack of visible changes of the position of absorption band of this compound when the solvent polarity is changed. We can see that introduction of the electrodonating group (dimethylamine) causes a rise of the dipole moment in the ground state of molecules **II** and **III**.

As mentioned previously we analysed the band shape of the charge transfer fluorescence of **II** and **III** in terms of modern electron transfer theory for radiative CT processes. An example of the fit is presented in Fig. 9.

We expect that increasing solvent polarity should cause an increase of the external reorganization energy and a decrease of the energy gap between the charge transfer and the ground

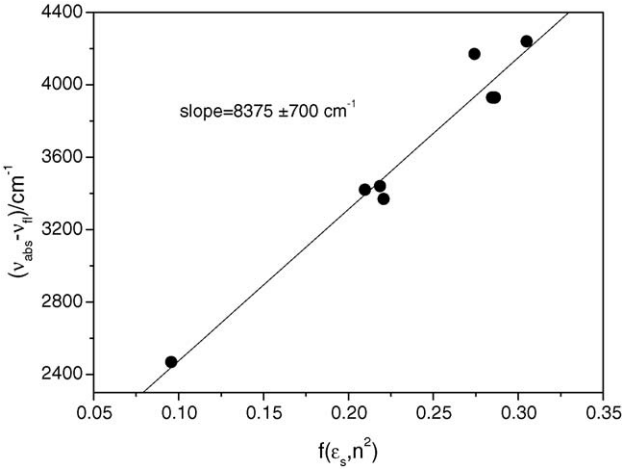

Fig. 8. Dependence of the difference of the positions of the maximum of the CT absorption and fluorescence on the solvent polarity function $f(\varepsilon_s, n^2) = ((\varepsilon_s - 1)/(2\varepsilon_s + 1) - (n^2 - 1)/(2n^2 + 1))$ for the compound **II**.

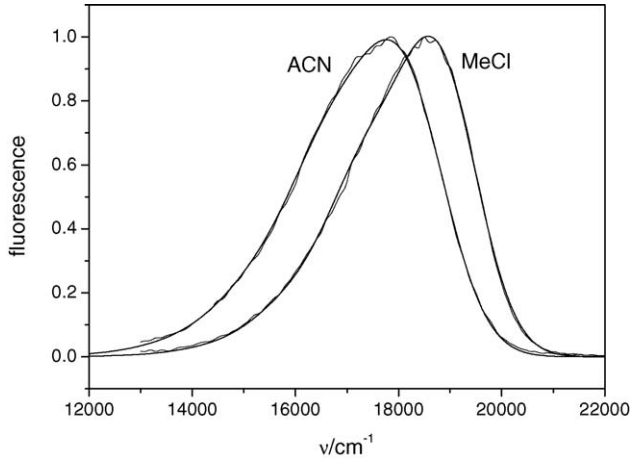

Fig. 9. CT fluorescence spectra of compound **II** in acetonitrile and methylene dichloride and their predictions given by Eq. (5). The fitted parameters were: $\Delta G_{et} = -2.44\,(-2.47)$ eV, $\lambda_s = 0.22\,(0.198)$ eV, $\lambda_v = 0.137$ eV for acetonitrile and methylene dichloride (in parentheses), respectively. The errors of the estimated parameters are for $MeCl_2$: ΔG_{et} (0.06) and λ_s (0.02) and in acetonitrile 0.08 and 0.02 for ΔG_{et} and λ_s, respectively. For λ_v the error for all the investigated systems does not exceed 0.04.

states. Indeed, the solvent reorganization energy increases with increasing solvent polarity as it is demonstrated in Fig. 10.

Similarly, the energy gap as a function of the solvent polarity function is plotted in Fig. 11.

This result is in reasonable agreement with the predictions given by the following equation [5]:

$$\Delta G_{CT} = \Delta G_{CT}(\text{vacuum}) - \frac{\vec{\mu}_e^2 - \vec{\mu}_g^2}{4\pi\varepsilon_0 a^3}\left(\frac{\varepsilon_s - 1}{2\varepsilon_s + 1}\right) \quad (7)$$

where ΔG_{CT}(vacuum) is the free enthalpy change extrapolated to the gas phase. The other parameters appearing in the above equation were defined previously. This equation predicts the reduction of the energy gap when solvent polarity increases. Analogous behaviours are found for compound **III**. Again, we observe increasing of the reorganization energy and reduction

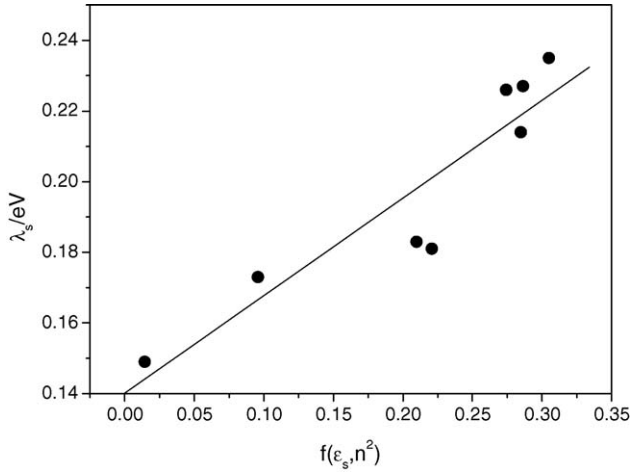

Fig. 10. Dependence of the experimentally obtained solvent reorganization energy (CT fluorescence analysis) of the compound **II** on the solvent polarity parameter, $f(\varepsilon_s, n^2) = ((\varepsilon_s - 1)/(2\varepsilon_s + 1) - (n^2 - 1)/(2n^2 + 1))$.

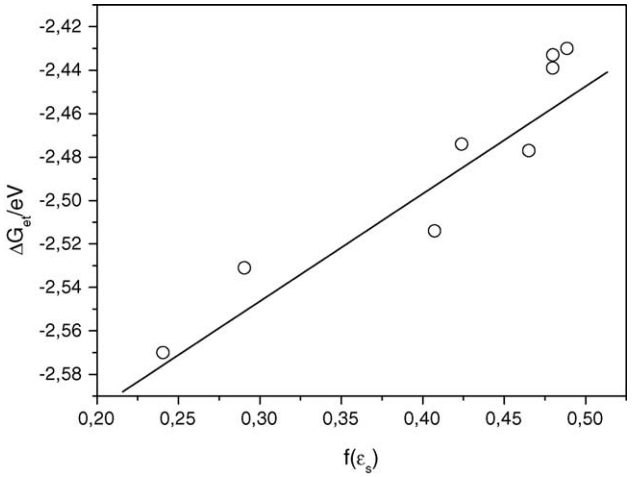

Fig. 11. Solvent polarity dependence of free enthalpy changes for the process $^1CT \Rightarrow S_0$ for **II** at 293 K. The solvent polarity function ($f(\varepsilon_s)$) is equal to $(\varepsilon_s - 1)/(2\varepsilon_s + 1)$. The values of ΔG_{et} were obtained from charge transfer fluorescence band analysis according to Eq. (5) (see Section 2—calculations).

of the energy gap between the CT and the ground state due to increasing solvent polarity.

The results of the similar analysis for the substance **III** are presented in Table 2 and lead to the following conclusions.

The important difference between **II** and **III** is a smaller energy gap between the CT and ground states for **III**, it corresponds also to the smaller excitation energy for compound **III** as compared to that of **II**. We observe also somewhat larger external reorganization energy for **III** as compared to **II**, especially in solvents of larger polarity. The results indicate strongly that the fluorescence emitting state of **II** and **III** has a charge transfer character.

All investigated molecules contain several functional groups (phenyl in all compounds and dimethylamine in **II** and **III**) which may undergo medium frequency vibrations (300–600 cm^{-1}) connected with medium frequency reorganization energy λ_L. Information about the relative contribution of the medium-frequency reorganization energy can be obtained from the analysis of temperature effects on charge transfer fluorescence.

We analysed then the temperature behaviour of the fluorescence spectra of **II** and **III** in solvents of different polarities

Table 2
Electron transfer parameters for the back electron transfer process recovered from the band shape analysis

Solvent	Compound **II**[a]		Compound **III**[b]	
	ΔG_{et} (eV)	λ_s (eV)	ΔG_{et} (eV)	λ_s (eV)
DBE	−2.631	0.173	−2.434	0.174
THF	−2.514	0.183	−2.52	0.188
EtBr	−2.549	0.182	−2.347	0.183
$MeCl_2$	−2.478	0.198	−2.30	0.195
Acetone	−2.478	0.214	−2.299	0.263
Acetonitrile	−2.439	0.220	−2.250	0.261
DMF	−2.433	0.226	−2.255	0.262
PC	−2.430	0.227	−2.251	0.263

[a] λ_{in}(averaged) = 0.137 eV.
[b] λ_{in}(averaged) = 0.125 eV

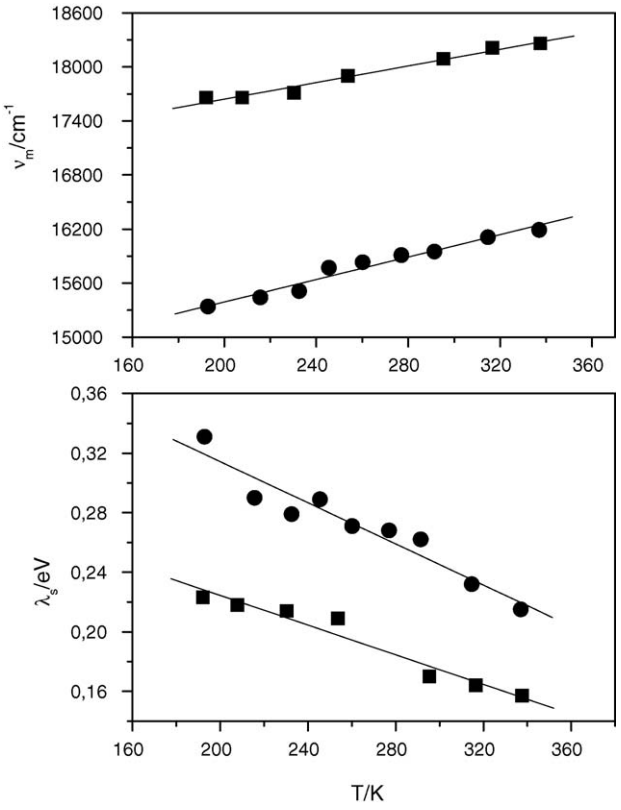

Fig. 12. Temperature dependence of the position of the maximum of CT fluorescence (top) and experimentally obtained (CT fluorescence band analysis) external reorganization energy (bottom) for **III** in DBE (squares) and DMF (circles).

(DMF and DBE) in respect of the electron transfer theory for radiative transitions (Eq. (5)). The results are plotted in Fig. 12.

Increasing temperature leads to the hypsochromic shifts of the CT fluorescence band maximum, this effect is called *thermochromic effect*.

The external reorganization energies decrease when temperature increases due to decrease of dielectric constant with increasing temperature. The thermochromic effect is observed for all investigated systems. Such behaviour was observed previously in the case of bianthryls in solvents of different polarities [15,22].

However, we do not observe the expected increase of the energy gap between the charge transfer and the ground states with an increase of temperature. Moreover, the changes of the recovered solvent reorganization energies are much more pronounced as expected on the basis of Eq. (4) (and the temperature dependence of the dielectric constant and refraction index of the solvents). The situation is similar to that observed for bianthryl derivative (10,10′dibromo, 9,9′-bianthryl) presented in the previous paper [22]. The two above-mentioned experimental facts indicate that the intramolecular motions of medium frequencies may be operative in the case of aminoderivatives of 1*H*-pyrazolo[3,4-*b*]quinoxalines.

Thus, we adopted an approach described by Cortes et al. [23] which includes the intramolecular modes (characterized by medium frequency $h\omega_L$) in the description of the electron transfer processes occurring here. In this case the CT fluorescence band shape has the following form:

$$\frac{\mathrm{CT}(\nu)}{\nu^3} = \sum_j \frac{S^j}{j!} \exp\left(-\frac{(\Delta G'_{et} + jh\omega_i + \lambda'_s + \lambda_L + h\nu)^2}{2(2\lambda'_s kT + \lambda_L h\varpi_L \coth(h\varpi_L/2kT))}\right) \quad (8)$$

where the symbols have similar meanings as those used in Eq. (5) except λ_L, λ'_s and $\Delta G'_{et}$. The last two parameters are the solvent reorganization energy and free enthalpy changes in the two intramolecular modes approximation, respectively. It should be noted that the new fits of Eq. (8) to the experimental data are not required but a simple reinterpretation of the previously obtained values of λ_s and ΔG_{et} is sufficient.

$$\lambda_s = \lambda'_s + \lambda_L \frac{h\omega_L}{2kT} \coth \frac{h\varpi_L}{2kT} \quad (8a)$$

$$\Delta G_s = \Delta G'_s - \lambda_L \left(\frac{h\omega_L}{2kT} \coth \frac{h\varpi_L}{2kT} - 1\right) \quad (8b)$$

where λ_L is the reorganization energy of the intermediate mode of frequency ω_L. To extract the values of λ'_s and $\Delta G'_{et}$ the linear dependence of λ_s as a function of $\coth(h\omega_L/2kT)$ is plotted in Fig. 13.

The slopes of the above-plotted dependencies are almost identical (the mean value is equal 0.09 eV) which corresponds to the medium frequency internal reorganization energy. The value of the medium frequency internal reorganization energy may be obtained also from the dependence of λ_s (estimated from the CT fluorescence band-shape analysis values). The linear plots of λ_s as a function of solvent polarity function gave the abscissas equal to 0.08 and 0.09 eV for **II** and **III**, respectively.

These results lead to the conclusion that in the description of the radiative back electron transfer processes the single-high frequency intramolecular model is not sufficient ($h\omega_i = 1600\,\mathrm{cm}^{-1}$) but an additional intramolecular mode of medium frequency ($600\,\mathrm{cm}^{-1}$) is required.

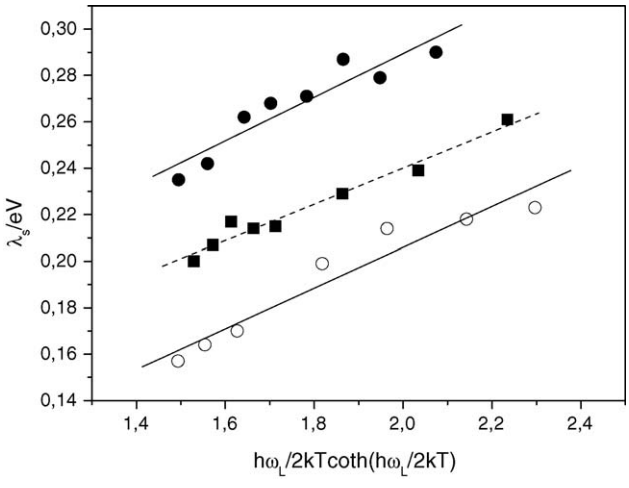

Fig. 13. Dependence of solvent reorganization energy λ_s, extracted from the fluorescence spectra on temperature dependent function $h\omega_L/2kT\coth(h\omega_L/2kT)$ for **II** in DMF (squares) and **III** in DBE (open circles) and in DMF (black circles). As a value of medium frequency motion the value of $600\,\mathrm{cm}^{-1}$ was assumed.

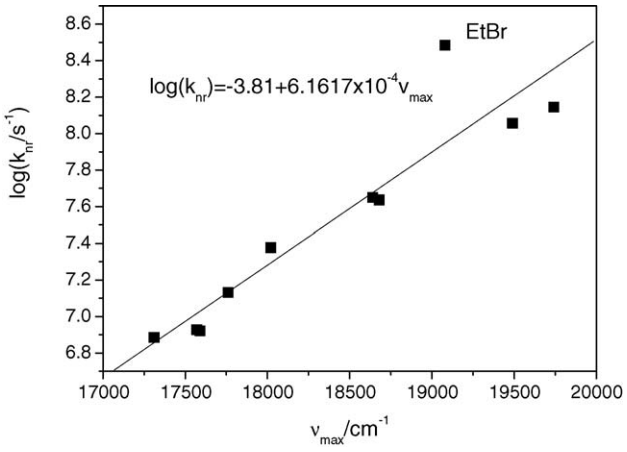

Fig. 14. Dependence of the radiationless transition rate constants k_{nr} (in logarithmic scale) on the spectral position of the CT fluorescence band maximum at room temperature for **II** in solvents of different polarities. The values of k_{nr} were calculated from the fluorescence quantum yields and lifetimes, $k_{nr} = (1 - \Phi_{fl})/\tau$.

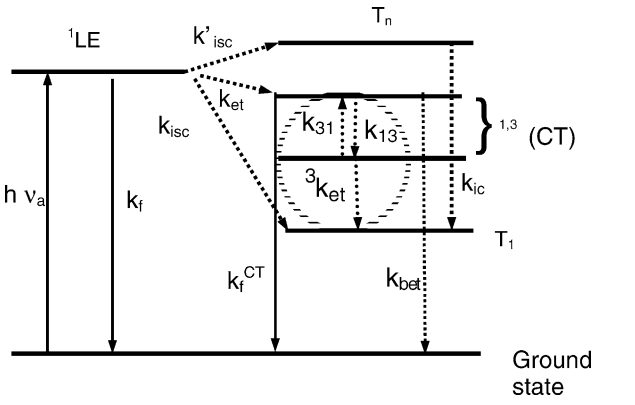

Scheme 3. Jabłonski diagram illustrating the photophysical processes occurring in investigated compounds after excitation to the excited singlet state of the molecule. Note, that in compounds **II** and **III** the emitting ^{1}CT state is populated directly, without intermediacy of the locally excited singlet state ^{1}LE in solvents other than *n*-hexane. In the oval the possible photophysical processes leading to the population of the lowest triplet (LE) state of the molecules from the charge transfer state are presented (route 'a'). The solid (broken) lines correspond to the radiative (nonradiative) transitions.

4.2. Radiationless transitions

As we can infer from Table 1 the fluorescence quantum yields and lifetimes depend strongly on solvent polarity, and more precisely on the position of the charge transfer fluorescence band maximum. It implies that the nonradiative transitions (including the ISC process) are also solvent polarity dependent. This behaviour is illustrated in Fig. 14 (as a dependence on the position of the CT fluorescence maximum).

To explain this fact let us consider the following Jablonski diagram, describing the photophysical processes occurring in the investigated compounds.

The flash photolysis experiments done with the investigated substances suggest that the lowest triplet state has an LE character, i.e. the two unpaired electrons are located somewhere in the pyrazoloquinoxaline ring and therefore it possesses the energy which is independent of the solvent polarity. To determine the triplet state energy we performed the low-temperature measurements. In solvents which do not contain a heavy atom (iodide) no low-temperature phosphorescence could be detected. We found phosphorescence for compounds **I** and **III** in ethyl iodide at 77 K. Estimated energy of the triplet state for **I** is 2.05 eV which is in agreement with the findings presented by Kucybala et al. [24] (equal to 2.06 eV). For **III** the position of the triplet state is ca. 1.88 eV.

The explanation of the intersystem crossing is as follows. From our previous papers [15,22] emerges that in the systems which exhibit the CT fluorescence (biaryls) the molecular triplet state populates via sequential spin inversion within charge transfer pair and monomolecular electron transfer process. Thus, we assumed this mechanism ($^1\text{CT} \Leftrightarrow {}^3\text{CT}$ followed by the spin allowed electron transfer process $^3\text{CT} \Rightarrow \text{T}_1$ (route 'a' in Scheme 3)) for our systems. In consequence, in the systems where the emitting CT state is lying highly above the molecular triplet state the most important deactivation route will be the intersystem crossing leading to the population of the molecular triplet state and the direct recombination to the ground state is negligible (molecule **II**). Assuming that the intramolecular electron transfer process $^1\text{LE} \Rightarrow {}^1\text{CT}$ is very fast (compound **I**) or the excitation leads directly to the ^{1}CT state (compounds **II** and **III**) the observed intersystem crossing rate constant can be approximated by the following equation:

$$k_{\text{isc}} = \frac{{}^3k_{\text{et}}k_{13}}{k_{31} + {}^3k_{\text{et}}} \tag{9}$$

where k_{13} and k_{31} correspond to the spin inversion rate constants $^1\text{CT} \Rightarrow {}^3\text{CT}$ and $^3\text{CT} \Rightarrow {}^1\text{CT}$, respectively, and $^3k_{\text{et}}$ is the rate constant of the spin allowed electron transfer process $^3\text{CT} \Rightarrow \text{T}_1$. When the later process is slower than the spin inversion $^3\text{CT} \Rightarrow {}^1\text{CT}$ then it becomes the rate-determining step and $k_{\text{isc}} \propto {}^3k_{\text{et}}$. In this case the intersystem crossing process will behave like the radiationless electron transfer process in the normal Marcus region with the appropriate consequences such as its dependence on solvent polarity and temperature. The ISC rate constant will be altered by the energy gap between the charge transfer and lowest triplet state (more precisely, between the ^{3}CT and T_1 states). We can expect that the rate constant of this process decreases with decreasing the energy gap between the above-mentioned states, thus the increasing solvent polarity causes decrease of the CT energy level (stabilizing the charge transfer state) and in consequence slows the intersystem crossing. However, the intersystem crossing competes with other deactivation processes of the CT state, such as radiative and nonradiative transitions which recover the ground state of the molecule. Deceleration of the ISC process makes the other deactivation routes more effective, thus significant increase of the fluorescence quantum yield and the lifetime of compound **II** in strongly polar solvents is observed.

Further lowering of the singlet CT state will however promote the recombination to the ground state of the molecules (molecule **III**). This process proceeds in the inverted Marcus region; it means that the rate constant increases with decreasing energy gap between the CT and the ground state. The larger

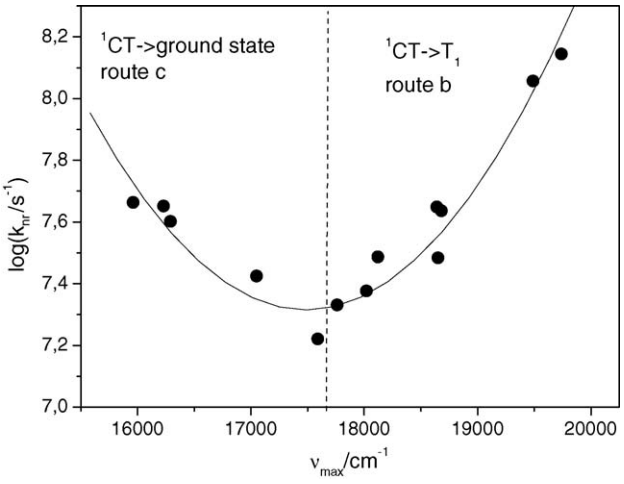

Fig. 15. Nature of radiationless transitions in compounds **II** and **III**. Dependence of the radiationless transition rate constants k_{nr} (in log scale) on the spectral position of the CT fluorescence band maximum at room temperature for **II** and **III** in solvents of different polarities. The solid line is drawn only to show the trend in the changes of these values. The values of k_{nr} were calculated from the fluorescence quantum yields and lifetimes, $k_{nr} = (1 - \Phi_{fl})/\tau$. Two routes of the nonradiative transitions are indicated, route 'b' where ISC process becomes dominating ($^1CT \Rightarrow T_1$) and route 'c' when direct recovering of the ground state is more important.

energy gap between the CT and ground states as in the case of the molecule **II** the less efficient the competition of the nonradiative back electron transfer (to the ground state) with the radiative and ISC processes. For the molecule **III** where this energy gap becomes smaller we should expect a certain contribution of the nonradiative back electron transfer to the overall deactivation of the CT state. Indeed, we observe some declination of the fluorescence quantum yield and the lifetime when the solvent polarity increases, but this effect is less pronounced than in the case of the compound **II**. Both cases can be described by a common dependence of the logarithm of the nonradiative transition rate constant on the energy of the CT state and should have a parabolic form with two distinctive regions (routes 'b' and 'c'). Such situation occurs as it is pointed out in Fig. 15.

If we assume that nonradiative transitions are the consequence of the electron transfer processes either to the triplet state (route 'b') or to the ground state (route 'c') then their rates should depend on the position of the CT state according to the Marcus theory.

The validity of this hypothesis may be verified by calculation of the electron transfer rate constants both from the ^{1}CT to the triplet (route 'b') and to the ground state (route 'c'). To do that we need to know one additional parameter characterizing the electron transfer process, namely the electronic coupling matrix element V. This may be done via estimation of the electronic transition dipole moment M_{fl}. The estimation of this parameter bases on a simple relation between the fluorescence rate constant k_{fl} and the averaged maximum of the charge transfer emission ν_{av} [25].

$$k_{fl} = \frac{\Phi_{fl}}{\tau_{fl}} = \frac{1}{3.1887 \times 10^6}(n\nu_{av})^3 M_{fl}^2 \tag{10}$$

where the averaged emission frequency is given by the equation [25]:

$$\nu_{av} = \frac{\int I(\nu)\nu \, d\nu}{\int I(\nu) \, d\nu} \tag{10a}$$

The absorption transition dipole moment can be calculated from the formula [25]:

$$M_{abs}^2 = 9.1853 \times 10^{-3} \frac{1}{n} \int \frac{\varepsilon(\nu)}{\nu} \, d\nu \tag{11}$$

The integral in Eq. (11) denotes the integrated reduced molar absorption and the constants in Eqs. (10) and (11) emerge from the simple calculations of the basic physical constants (Planck' and Avogadro's constants, velocity of light c, etc.).

We found that the transition dipole moment for absorption is equal 2.0 D for **II**, 2.7 D for **III** and 3.5 D for **I** and it seems to be solvent independent. The transition dipole moments for fluorescence seem to be solvent independent for **II** and **III** and equal to 3.5 ± 0.4 and 2.15 ± 0.2 D for these compounds, respectively. The difference of the transition dipole moment for absorption and fluorescence for the molecule **II** may indicate the conformational changes (flattening) of the molecule in the excited singlet state of **II**. However, the larger value of the transition dipole moment for **II** may indicate that the charge transfer state (emitting fluorescence) contains a contribution of the locally excited state (π,π^*) whereas for **III** the emitting charge transfer state does not contain such LE state contribution. Thus, only for the latter case the electronic coupling element V_0 between the CT and the ground state may be easily calculated from the relation [8]:

$$M_{fl} = V_0 \frac{\Delta\mu}{hc\nu_{CT}} \tag{12}$$

The value of the electronic coupling matrix element V_0 is equal 0.22 eV for **III** in the investigated solvents. Now we are able to calculate the values of the back electron transfer rate constants, corresponding to the recovering of the ground state according to the Jortner formula for nonadiabatic electron transfer process [26].

$$k_{et} = \sum_{j=0}^{\infty} \frac{2\pi V^2 \exp(-S) S^j / j!}{h(4\pi\lambda_s kT)^{1/2}} \exp\left(-\frac{(\Delta G + jh\Omega + \lambda_s)^2}{4\lambda_s kT}\right) \tag{13}$$

where the parameters occurring in the above equation have been defined previously. The results are presented in Fig. 16.

The lowering of the emitting CT singlet state causes the enhancement of the nonradiative back electron transfer rate constant which recovers the ground state of the compound. This observation is in agreement with the Marcus-type theory in the inverted region.

The electron transfer process leading to the population of the molecular triplet state proceeds in the normal Marcus region. For this process the theory predicts a decreasing rate constant with increasing ΔG. Thus for larger values of the energy of the CT state an enhancement of the radiationless transition is again

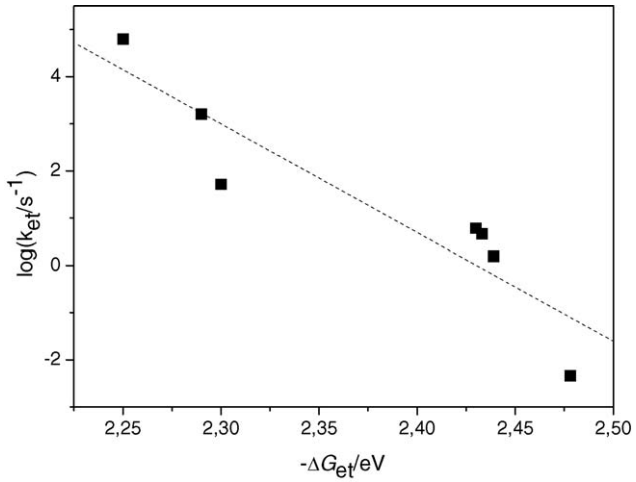

Fig. 16. Predicted values of the back electron transfer rate constant against the energy gap between the CT and the ground states of **III** at 293 K. The theoretical values were calculated according to Eq. (13) with the parameters collected in Table 2. The line is drawn only for presentation purpose.

observed. In this way the behaviour (increasing electron transfer rate constant with decreasing charge transfer fluorescence energy) illustrated in Fig. 15 may be explained.

The next question arises, how to explain why we do not observe the low-temperature phosphorescence? Let us assume that in the compound **I** the charge separation, if any, is not complete. Certainly, such situation occurs in nonpolar *n*-hexane. Steady-state temperature measurements of the compound **I** in *n*-hexane show that the fluorescence band shape is not affected by temperature, which indicates that the lowest singlet state has no charge transfer character. We suppose that the population of the lowest triplet state proceeds via higher lying triplet state, which location is close to the emitting singlet state. Thus, we performed the temperature measurements of the fluorescence lifetimes and quantum yields for this compound in *n*-hexane. From these data we found that the nonradiative transition rate constant is strongly temperature dependent as demonstrated in Fig. 17. The energy of activation, calculated from the Arrhenius plot is equal to 18.4 kJ/mol. Similar value was obtained for **II** in DBE (12.57 kJ/mol) (for this system the Arrhenius dependence was not a single exponential). At liquid nitrogen temperature this thermally activated process does not play an important role in deactivation of the singlet state and consequently phosphorescence is not observed. In ethyl iodide at 77 K, however, the 'direct' $^1LE \Rightarrow T_1$ intersystem crossing is possible due to external heavy atom perturbation. This may explain the occurrence of low-temperature phosphorescence of **I** and **III** in frozen ethyl iodide solution.

Surprisingly, in acetonitrile the nonradiative transitions are more effective when temperature decreases. One possible explanation is following.

After excitation to the locally excited singlet state an efficient electron transfer process occurs in **I** even in strongly polar acetonitrile. It leads to the radical pair which may recombine to its ground or triplet states. The first process is governed by the Marcus rule for the nonradiative electron transfer process in the inverted region. In this case the back electron transfer process depends on solvent polarity, more exactly this process is strongly accelerated in polar solvents. Moreover, for the electron transfer processes occurring in the inverted Marcus region, the theory predicts a decrease of the radiationless transition rate constant with increasing temperature, because increasing temperature causes a decrease of the solvent reorganization energy. This effect is presented in Fig. 18. The analysis of the fluorescence spectra of **I** in polar solvents such as acetone, DMF, PC and acetonitrile yields the values of λ_s, λ_v and ΔG_{et} around 0.3, 0.35, and −2.7 eV, respectively.

Therefore, decreasing temperature causes an increase of the rate of the nonradiative transition leading to the ground state recovery. As mentioned above this process is a dominating pathway in deactivation of the excited singlet state (very weak intersystem crossing is observed in polar solvents).

The nature of the electronic states in the compounds **I**, **II** and **III** seems to be as follows.

The first singlet state of **I** is a π,π^* state, because the molar absorption coefficients for the transition from the ground state are in the range of 6000 mol^{-1} cm^{-1} dm^3, whereas for the

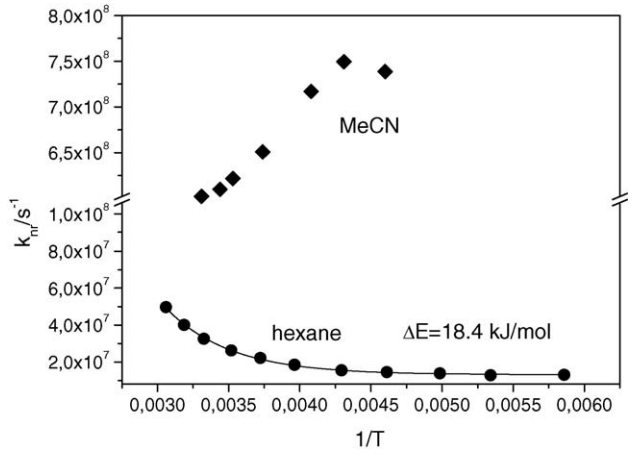

Fig. 17. Arrhenius plot for nonradiative deactivation rate constant of **I** in *n*-hexane and acetonitrile.

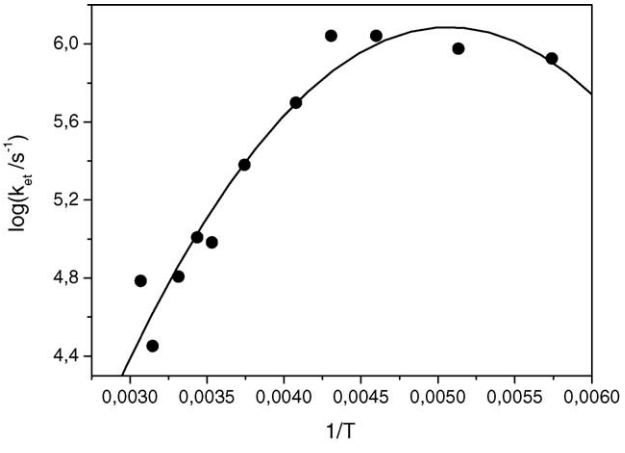

Fig. 18. Predicted values of the back electron transfer rate constant of **I** in acetonitrile as a function of temperature. The calculations were done using Eq. (13) with the parameters obtained from the CT fluorescence band shape analysis.

compounds **II** and **III** the lowest singlet state has a charge transfer character (at least in solvents more polar than DBE—cf. Fig. 2)). Moreover, the absorption of **I** in polar solvents (acetonitrile) is not affected by a presence of small amounts of sulphuric acid whereas this presence strongly affects the absorption of **II** and **III**.[1] Additionally, it is commonly known that the fluorescence does not occur from the n,π* states, whereas for our compounds relatively intense fluorescence is observed (Table 1). The lowest triplet state has the same symmetry (π,π*) because the singlet–triplet split is of the order of 6500 cm^{-1}, and in addition the band shape of the absorption $T_1 \Rightarrow T_n$ is independent of the solvent polarity. Thus, according to the El Sayed rule the direct transition $^1LE \Rightarrow T_1$ (intersystem crossing) should be strongly prohibited [27]. However, in the vicinity of the first excited singlet state another triplet state can be thermally populated, this may be a state of the n,π* symmetry. Such a situation occurs in nonpolar solvents. In polar solvents where CT state is populated (via intramolecular charge transfer process or via direct excitation) the spin inversion and further recombination of the ^3CT state does not lead to the molecular triplet state. The possible explanation is that the electron transfer process ($^3CT \Rightarrow T_1$) occurs in the normal Marcus region where decreasing the energy gap leads to decrease of the electron transfer rate constant.

However, there may be an alternative explanation of the deceleration of the intersystem crossing in polar solvents which is observed in all investigated compounds. The intersystem crossing occurs only from the LE state, which is of the π,π* symmetry. Previously we have assumed that the emitting state is a 'pure' charge transfer state. It may be true only in polar solvents. Although the lowest singlet state of the compounds **II** and **III** indicates the behaviours which are characteristic for the CT state the, the CT singlet state may possess some character of the closely lying locally excited state (cf. Fig. 2). Thus the wavefunction of the first excited singlet state has a form [28]:

$$\Phi(\mathrm{CT}) = \Phi^0(\mathrm{CT}) + \beta\Phi^0(\mathrm{LE}) = \Phi^0(\mathrm{CT}) + \frac{\left|\langle \mathrm{CT}|\,\hat{H}\,|\mathrm{LE}\rangle\right|}{|E_{\mathrm{CT}} - E_{\mathrm{LE}}|}\Phi^0(\mathrm{LE}) \quad (14)$$

As can be seen from the above equation the mixing of the pure CT and LE states depends on the energy gap between the CT and LE states. The increasing solvent polarity causes an increase of the energy gap and then the contribution of the LE state to the lowest excited singlet state decreases. If we assume now that the intersystem crossing occurs between the pure LE state and the higher triplet state having different symmetry (according to the El Sayed rule) we have a possible explanation of the reduction of the triplet state population in polar solvents.

This is schematically depicted in Scheme 4.

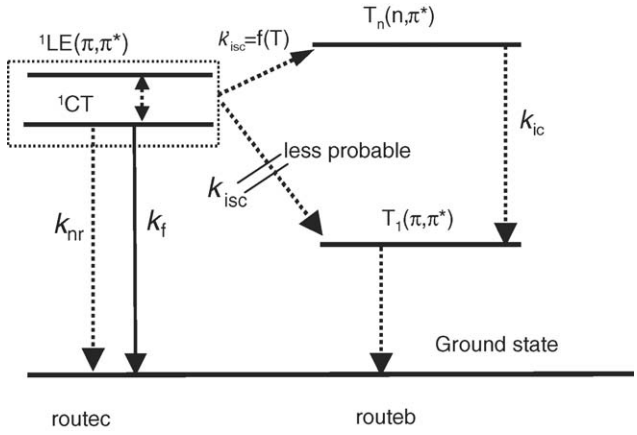

Scheme 4. Nature of radiationless transition in investigated compounds. The mixing of the single states is indicated by rectangle. For compound **II** the intersystem crossing $^1CT \Rightarrow T_n \Rightarrow T_1$ is the important deactivation pathway (route 'b') whereas for compound **III** a direct $^1CT \Rightarrow$ ground state becomes more important (route 'c'). A direct $^1CT \Rightarrow T_1$ intersystem crossing process seems to be unimportant.

5. Conclusions

The fluorescence behaviour of 1*H*-pyrazolo[3,4-*b*]quinoxaline derivatives was investigated in solvents of different polarities and at different temperatures. We found that in all the investigated molecules the fluorescence occurs from the singlet state which possesses the charge transfer character. The fluorescence band shape analysis supports the concept of the decreasing energy gap between the CT and the ground states and the increasing solvent reorganization energy when the solvent polarity increases. It seems that the intramolecular modes of intermediate frequencies (ca. 600 cm^{-1}) make a significant contribution to the overall intramolecular rearrangement. It may be a torsional mode of the amino group connected to the 1*H*-pyrazolo[3,4-*b*]quinoxaline ring.

The deactivation pathways of the singlet excited state of the investigated compounds are: the fluorescence, the intersystem crossing leading to the population of the molecular triplet state and the internal conversion leading to the recovery of the ground state. In polar solvents this third route seems to be very important in qualitative agreement with the Marcus theory for the radiationless electron transfer transition (molecules **I** and **III**).

Comparison of the fluorescence and absorption behaviour of **II** and **III** indicates an important difference between the two compounds. Formally, the two compounds are isomers in which the dimethylamino group is connected at different positions. If we assume that the position of the charge transfer state is determined by the electron donating and accepting properties of the donor (dimethylamine) and acceptor (1*H*-pyrazolo[3,4-*b*]quinoxaline) the absorption and fluorescence spectra should be very similar to each other. Certainly, we have a different situation. The energy of the charge transfer state may be calculated from the oxidation potential of dimethylamine and the reduction potential of 1*H*-pyrazolo[3,4-*b*]quinoxaline. Assuming the values of redox potentials as 1.31 V [29] and −1.134 V [24], we obtain the value of 2.44 eV in acetonitrile. This result is in

[1] Addition of sulphuric acid as well as the presence of methanol affect strongly the fluorescence of **I** where the very effective fluorescence quenching is observed. These effects will be described in an additional paper.

excellent agreement with our estimation of the CT state energy of **II** in acetonitrile (cf. Table 2), but it is too high for **III** in acetonitrile (2.25 eV). It means that only the first compound (**II**) may be treated as the sum of the independent components (donor and acceptor subunits).

Acknowledgements

This work was supported by the State Committee of Scientific Research of Poland (Grants No. 3 T09A 102 18 and 4T09A 109 25). We would like to thank Prof. Jan Najbar for diverse help in the course of completion of this project and Dr. Andrzej M. Turek for editorial comments.

References

[1] A. Kapturkiewicz, J. Herbich, J. Karpiuk, J. Nowacki, J. Phys. Chem. A 101 (1997) 2332.
[2] J. Herbich, A. Kapturkiewicz, Chem. Phys. Lett. 273 (1997) 8.
[3] R. Czerwieniec, J. Herbich, A. Kapturkiewicz, J. Nowacki, Chem. Phys. Lett. 325 (2000) 589.
[4] P. Borowicz, J. Herbich, A. Kapturkiewicz, J. Nowacki, Chem. Phys. 244 (1999) 251.
[5] P. Borowicz, J. Herbich, A. Kapturkiewicz, J. Nowacki, M. Opallo, Chem. Phys. 249 (1999) 49.
[6] T. Yoshihara, V.A. Galievsky, S.I. Druzhinin, S. Saha, K.A. Zachariasse, Photochem. Photobiol. Sci. 2 (2003) 342.
[7] T. von der Haar, A. Hebecker, Y.V. Il'ichev, Y.-B. Jiang, W. Kühnle, K.A. Zachariasse, Rec. Trav. Chim. Pays-Bas 114 (1995) 430.
[8] J. Herbich, A. Kapturkiewicz, J. Am. Chem. Soc. 120 (1998) 1014.
[9] Y.V. Il'ichev, W. Kühnle, K.A. Zachariasse, Chem. Phys. 211 (1996) 441.
[10] J. Herbich, A. Kapturkiewicz, J. Nowacki, J. Goliński, Z. Dąbrowski, Phys. Chem. Chem. Phys. 3 (2001) 2438.
[11] L.S. Hung, C.H. Chen, Mater. Sci. Eng. R 39 (2002) 143.
[12] R.A. Marcus, J. Phys. Chem. 93 (1989) 3078.
[13] I.R. Gould, S. Farid, J. Photochem. Photobiol. A: Chem. 65 (1992) 133.
[14] M. Schütz, R. Schmidt, J. Phys. Chem. 100 (1996) 2012.
[15] M. Mac, P. Milart, P. Kwiatkowski, B. Tokarczyk, J. Lumin. 81 (1999) 199;
M. Mac, P. Kwiatkowski, U. Pischel, Chem. Phys. Lett. 357 (2002) 440;
M. Mac, A. Danel, K. Kizior, P. Nowak, A. Karocki, B. Tokarczyk, Phys. Chem. Chem. Phys. 5 (2003) 988.
[16] J. Herbich, A. Kapturkiewicz, Chem. Phys. 170 (1993) 221.
[17] I.R. Gould, R.H. Young, L.J. Mueller, A.C. Albrecht, S. Farid, J. Am. Chem. Soc. 116 (1994) 8188;
I.R. Gould, R.H. Young, R.E. Moody, S. Farid, J. Phys. Chem. 95 (1991) 2068.
[18] P. Wang, Z. Xie, Z. Hong, J. Tang, O. Wong, Ch.-S. Lee, N. Wong, S. Lee, J. Mater. Chem. 13 (2003) 1894.
[19] G.B. Bacon, S.D. Hamilton, J. Chem. Soc. Perkin (1974) 1965.
[20] M.A. Khan, A.C.C. Freitas, J. Heter. Chem. 20 (1983) 277.
[21] E. Lippert, Z. Naturforsch. 10a (1955) 541;
N. Mataga, Y. Kaifu, M. Koizumi, Bull. Chem. Soc. Jpn. 28 (1955) 690.
[22] M. Mac, A. Danel, A. Michno, R. Krolicki, J. Lumin., in press.
[23] J. Cortes, H. Heitele, J. Jortner, J. Phys. Chem. 98 (1994) 2527.
[24] Z. Kucybala, A. Kossobucka, J. Paczkowski, J. Photochem. Photobiol. A: Chem. 136 (2000) 227.
[25] J.E. Lewis, M. Maroncelli, Chem. Phys. Lett. 282 (1998) 197.
[26] J. Jortner, J. Chem. Phys. 64 (1976) 4860.
[27] M. ElSayed, J. Chem. Phys. 38 (1963) 2834;
R.S. Becker, Theory and Interpretation of Fluorescence and Phosphorescence, Wiley–Interscience, New York, 1969, pp. 155–189.
[28] N.J. Turro, Modern, Molecular Photochemistry, The Benjamin/Cummings Publishing Co. Inc., 1978 (Chapter 5).
[29] P. Jacques, X. Allonas, J. Photochem. Photobiol. A: Chem. 78 (1994) 1.